AMERICAN SOCIETY FOR MICROBIOLOGY | Molecular and Cellular Biology

Oma1 Links Mitochondrial Protein Quality Control and TOR Signaling To Modulate Physiological Plasticity and Cellular Stress Responses

Iryna Bohovych,[a,b] Stavroula Kastora,[c] Sara Christianson,[a] Danelle Topil,[a] Heejeong Kim,[a,b] Teresa Fangman,[b] You J. Zhou,[b] Antoni Barrientos,[d,e] Jaekwon Lee,[a,b] Alistair J. P. Brown,[c] Oleh Khalimonchuk[a,b]

Department of Biochemistry[a] and Redox Biology Center,[b] University of Nebraska—Lincoln, Lincoln, Nebraska, USA; School of Medical Sciences, University of Aberdeen, Foresterhill, Aberdeen, United Kingdom[c]; Department of Biochemistry and Molecular Biology[d] and Department of Neurology,[e] University of Miami School of Medicine, Miami, Florida, USA

A network of conserved proteases known as the intramitochondrial quality control (IMQC) system is central to mitochondrial protein homeostasis and cellular health. IMQC proteases also appear to participate in establishment of signaling cues for mitochondrion-to-nucleus communication. However, little is known about this process. Here, we show that in *Saccharomyces cerevisiae*, inactivation of the membrane-bound IMQC protease Oma1 interferes with oxidative-stress responses through enhanced production of reactive oxygen species (ROS) during logarithmic growth and reduced stress signaling via the TORC1-Rim15-Msn2/Msn4 axis. Pharmacological or genetic prevention of ROS accumulation in Oma1-deficient cells restores this defective TOR signaling. Additionally, inactivation of the Oma1 ortholog in the human fungal pathogen *Candida albicans* also alters TOR signaling and, unexpectedly, leads to increased resistance to neutrophil killing and virulence in the invertebrate animal model *Galleria mellonella*. Our findings reveal a novel and evolutionarily conserved link between IMQC and TOR-mediated signaling that regulates physiological plasticity and pancellular oxidative-stress responses.

Mounting evidence indicates that mitochondrial processes are tightly integrated with cellular signaling pathways (1–3). Such integration enables rapid modulation of mitochondrial functions upon homeostatic fluctuations in the intra- and extracellular environment and adaptation of cellular metabolism in response to changes within the mitochondrion. Studies in *Saccharomyces cerevisiae* have been instrumental for the elucidation of evolutionarily conserved aspects of mitochondrion-linked signaling. These analyses also provided insights into the mechanisms by which cells in general and mitochondria in particular are protected from oxidative insults (4).

Reactive oxygen species (ROS), a by-product of mitochondrial respiration, can damage a number of biological molecules, thereby affecting mitochondrial and cellular well-being (5, 6). Accumulating ROS-elicited oxidative stress and damage have long been known to be detrimental factors in many pathologies and aging (5, 7, 8). On the other hand, many ROS are now recognized as signaling molecules essential in multiple pathways, including mitochondrion-nucleus communication and longevity regulation (2, 6). The phenomenon, known as ROS adaptation, preconditioning, or hormesis, is believed to be one of the ways by which reduced signaling via the TOR pathway leads to stress-protective effects (2, 9). This effect partly stems from the derepression, through TOR inhibition, of the downstream signaling branch of the TOR pathway that includes the kinase Rim15 and a stress/nutrient signaling node containing the transcription factors Gis1 and the functionally redundant Msn2/Msn4 pair (4, 10). ROS adaptation requires respiration and is temporally restricted to logarithmic and diauxic growth phases (11).

A network of conserved proteases known as intramitochondrial quality control (IMQC) is central to normal mitochondrial activities (12). Studies in *S. cerevisiae* established that a specific IMQC protease, Oma1, is important in mitochondrial stress tolerance (13). This ATP-independent protease resides in the inner mitochondrial membrane (IM) as a high-mass complex and is dormant under physiological conditions (13–16). Conditions of mitochondrial stress, including acute treatment with H_2O_2 or respiratory uncoupling, lead to rapid activation of Oma1 through destabilization of the Oma1 oligomer (13, 16). Consistent with the protease's stress response role, yeast cells lacking functional Oma1 are vulnerable to oxidative stress (13). However, in the context of cellular physiology, it remains unclear how Oma1 promotes resistance to oxidative insults.

Here, using the *S. cerevisiae* model, we demonstrate that loss of Oma1 leads to elevated ROS production during active growth. Genetic and biochemical analyses indicate that ROS emitted by Oma1-deficient mitochondria act as an adaptation signal that impinges on the conserved TORC1-Rim15-Msn2/Msn4 signaling pathway regulating stress survival responses. In addition, we show that inactivation of the Oma1 ortholog in the human fungal pathogen *Candida albicans* also modulates TOR signaling. This unexpectedly promotes survival of the pathogen in human neutrophils and enhances its virulence. Our findings reveal a novel link between IMQC and ROS-modulated TOR signaling in the

Received 15 March 2016 **Returned for modification** 5 April 2016
Accepted 9 June 2016

Accepted manuscript posted online 20 June 2016

Citation Bohovych I, Kastora S, Christianson S, Topil D, Kim H, Fangman T, Zhou YJ, Barrientos A, Lee J, Brown AJP, Khalimonchuk O. 2016. Oma1 links mitochondrial protein quality control and TOR signaling to modulate physiological plasticity and cellular stress responses. Mol Cell Biol 36:2300–2312. doi:10.1128/MCB.00156-16.

Address correspondence to Oleh Khalimonchuk, okhalimonchuk2@unl.edu.

Copyright © 2016, American Society for Microbiology. All Rights Reserved.

Downloaded from http://mcb.asm.org/ on September 9, 2016 by University of Aberdeen

TABLE 1 Genotypes and sources of yeast strains used in this study

Strain or key element(s)	Genotype	Reference or source
W303-1B	*MAT*α *ade2-1 his3-1,15 leu2-3,112 trp1-1 ura3-1*	D. Winge
W303-2A	*MAT***a** *ade2-1 his3-1,15 leu2-3,112 trp1-1 ura3-1*	A. Barrientos
*oma1*Δ	*MAT*α *ade2-1 his3-1,15 leu2-3,112 trp1-1 ura3-1 oma1*Δ::*TRP1*	13
WT [*rho*^{0}]	*MAT*α *ade2-1 his3-1,15 leu2-3,112 trp1-1 ura3-1* [*rho*^{0}]	This study
*oma1*Δ [*rho*^{0}]	*MAT*α *ade2-1 his3-1,15 leu2-3,112 trp1-1 ura3-1 oma1*Δ::*TRP1* [*rho*^{0}]	This study
*tor1*Δ	*MAT***a** *ade2-1 his3-1,15 leu2-3,112 trp1*Δ *ura3-1 tor1*Δ::*kanMX4*	A. Barrientos
*tor1*Δ *oma1*Δ	*MAT***a** *ade2-1 his3-1,15 leu2-3,112 trp1*Δ *ura3-1 tor1*Δ::*kanMX4 oma1*Δ::*URA3MX*	This study
*yme1*Δ	*MAT*α *ade2-1 his3-1,15 leu2-3,112 trp1-1 ura3-1 yme1*Δ::*HIS3MX6*	13
*yme1*Δ *oma1*Δ	*MAT*α *ade2-1 his3-1,15 leu2-3,112 trp1-1 ura3-1 yme1*Δ::*HIS3MX6 oma1*Δ::*CaURA3*	13
*yta10*Δ	*MAT*α *ade2-1 his3-1,15 leu2-3,112 trp1-1 ura3-1 yta10*Δ::*HIS3*	D. Winge
*yta10*Δ *oma1*Δ	*MAT*α *ade2-1 his3-1,15 leu2-3,112 trp1-1 ura3-1 yta10*Δ::*HIS3MX6 oma1*Δ::*TRP1*	13
*pcp1*Δ	*MAT*α *ade2-1 his3-1,15 leu2-3,112 trp1-1 ura3-1 pcp1*Δ::*TRP1*	13
*pcp1*Δ *oma1*Δ	*MAT*α *ade2-1 his3-1,15 leu2-3,112 trp1-1 ura3-1 pcp1*Δ::*TRP1 oma1*Δ::*URA3MX*	13
*cox5a*Δ	*MAT*α *ade2-1 his3-1,15 leu2-3,112 trp1-1 ura3-1 1 cox5a*Δ::*HIS3*	D. Winge
*cox5a*Δ *oma1*Δ	*MAT*α *ade2-1 his3-1,15 leu2-3,112 trp1-1 ura3-1 1 cox5a*Δ::*HIS3 oma1*Δ::*CaURA3*	This study
*sch9*Δ	*MAT***a** *ade2-1 his3-1,15 leu2-3,112 trp1*Δ *ura3-1 sch9*Δ::*kanMX4*	A. Barrientos
*sch9*Δ *oma1*Δ	*MAT***a** *ade2-1 his3-1,15 leu2-3,112 trp1*Δ *ura3-1 sch9*Δ::*kanMX4 oma1*Δ::*URA3MX*	This study
*sch9*Δ *oma1*Δ *tor1*Δ	*MAT***a** *ade2-1 his3-1,15 leu2-3,112 trp1*Δ *ura3-1 sch9*Δ::*kanMX4 oma1-*Δ *tor1*Δ::*URA3MX*	This study
*rtg1*Δ	*MAT***a** *ade2-1 his3-1,15 leu2-3,112 trp1*Δ *ura3-1 rtg1*Δ::*TRP1*	This study
*rtg1*Δ *oma1*Δ	*MAT***a** *ade2-1 his3-1,15 leu2-3,112 trp1*Δ *ura3-1 rtg1*Δ::*TRP1 oma1*Δ::*URA3MX*	This study
*rtg2*Δ	*MAT***a** *ade2-1 his3-1,15 leu2-3,112 trp1*Δ *ura3-1 rtg2*Δ::*URA3MX*	This study
*rtg2*Δ *oma1*Δ	*MAT***a** *ade2-1 his3-1,15 leu2-3,112 trp1*Δ *ura3-1 rtg2-*Δ *oma1*Δ::*URA3MX*	This study
*ras2*Δ	*MAT***a** *ade2-1 his3-1,15 leu2-3,112 trp1*Δ *ura3-1 ras2*Δ::*URA3MX*	This study
*ras2*Δ *oma1*Δ	*MAT***a** *ade2-1 his3-1,15 leu2-3,112 trp1*Δ *ura3-1 ras2-*Δ *oma1*Δ::*URA3MX*	This study
*pde2*Δ	*MAT***a** *ade2-1 his3-1,15 leu2-3,112 trp1*Δ *ura3-1 pde2*Δ::*URA3MX*	This study
*pde2*Δ *oma1*Δ	*MAT***a** *ade2-1 his3-1,15 leu2-3,112 trp1*Δ *ura3-1 pde2-*Δ *oma1*Δ::*URA3MX*	This study
*avo2*Δ	*MAT***a** *ade2-1 his3-1,15 leu2-3,112 trp1*Δ *ura3-1 avo2*Δ::*URA3MX*	This study
*avo2*Δ *oma1*Δ	*MAT***a** *ade2-1 his3-1,15 leu2-3,112 trp1*Δ *ura3-1 avo2-*Δ *oma1*Δ::*URA3MX*	This study
*rim15*Δ	*MAT***a** *ade2-1 his3-1,15 leu2-3,112 trp1*Δ *ura3-1 rim15*Δ::*TRP1*	This study
*rim15*Δ *oma1*Δ	*MAT***a** *ade2-1 his3-1,15 leu2-3,112 trp1*Δ *ura3-1 rim15*Δ::*TRP1 oma1*Δ::*URA3MX*	This study
*gis1*Δ	*MAT***a** *ade2-1 his3-1,15 leu2-3,112 trp1*Δ *ura3-1 gis1*Δ::*URA3MX*	This study
*gis1*Δ *oma1*Δ	*MAT***a** *ade2-1 his3-1,15 leu2-3,112 trp1*Δ *ura3-1 gis1-*Δ *oma1*Δ::*URA3MX*	This study
*msn2*Δ	*MAT***a** *ade2-1 his3-1,15 leu2-3,112 trp1*Δ *ura3-1 msn2*Δ::*URA3MX*	This study
*msn4*Δ	*MAT***a** *ade2-1 his3-1,15 leu2-3,112 trp1*Δ *ura3-1 msn4*Δ::*URA3MX*	This study
*msn2*Δ *oma1*Δ	*MAT***a** *ade2-1 his3-1,15 leu2-3,112 trp1*Δ *ura3-1 msn2-*Δ *oma1*Δ::*URA3MX*	This study
*msn4*Δ *oma1*Δ	*MAT***a** *ade2-1 his3-1,15 leu2-3,112 trp1*Δ *ura3-1 msn4-*Δ *oma1*Δ::*URA3MX*	This study
*msn2*Δ *msn4*Δ	*MAT***a** *ade2-1 his3-1,15 leu2-3,112 trp1*Δ *ura3-1 msn4-*Δ *msn2*Δ::*URA3MX*	This study
*msn2*Δ *msn4*Δ *oma1*Δ	*MAT***a** *ade2-1 his3-1,15 leu2-3,112 trp1*Δ *ura3-1 msn4-*Δ *msn2-*Δ *oma1*Δ::*URA3MX*	This study
*pph21*Δ	*MAT***a** *ade2-1 his3-1,15 leu2-3,112 trp1*Δ *ura3-1 pph21*Δ::*URA3MX*	This study
*pph22*Δ	*MAT***a** *ade2-1 his3-1,15 leu2-3,112 trp1*Δ *ura3-1 pph22*Δ::*URA3MX*	This study
*pph21*Δ *oma1*Δ	*MAT***a** *ade2-1 his3-1,15 leu2-3,112 trp1*Δ *ura3-1 pph21-*Δ *oma1*Δ::*URA3MX*	This study
*pph22*Δ *oma1*Δ	*MAT***a** *ade2-1 his3-1,15 leu2-3,112 trp1*Δ *ura3-1 pph22-*Δ *oma1*Δ::*URA3MX*	This study
*pph21*Δ *pph22*Δ *oma1*Δ	*MAT***a** *ade2-1 his3-1,15 leu2-3,112 trp1*Δ *ura3-1 pph22-*Δ *pph21-*Δ *oma1*Δ::*URA3MX*	This study
*sch9*Δ *oma1*Δ [*rho*^{0}]	*MAT***a** *ade2-1 his3-1,15 leu2-3,112 trp1*Δ *ura3-1 sch9*Δ::*kanMX4 oma1*Δ::*URA3MX* [*rho*^{0}]	This study
*tor1*Δ *oma1*Δ [*rho*^{0}]	*MAT***a** *ade2-1 his3-1,15 leu2-3,112 trp1*Δ *ura3-1 tor1*Δ::*kanMX4 oma1*Δ::*URA3MX* [*rho*^{0}]	This study
*rim15*Δ *oma1*Δ [*rho*^{0}]	*MAT***a** *ade2-1 his3-1,15 leu2-3,112 trp1*Δ *ura3-1 rim15*Δ::*TRP1 oma1*Δ::*URA3MX* [*rho*^{0}]	This study
Npr1-3HA	*MAT***a** *ade2-1 his3-1,15 leu2-3,112 trp1*Δ *ura3-1 NPR1-3HA::klTRP1*	This study
*oma1*Δ *Npr1-3HA*	*MAT***a** *ade2-1 his3-1,15 leu2-3,112 trp1*Δ *ura3-1 NPR1-3HA::klTRP1 oma1*Δ::*URA3MX*	This study
*tor1*Δ *Npr1-3HA*	*MAT***a** *ade2-1 his3-1,15 leu2-3,112 trp1*Δ *ura3-1 NPR1-3HA::klTRP1 tor1*Δ::*URA3MX*	This study

regulation of physiological plasticity and pancellular stress responses.

MATERIALS AND METHODS

Yeast strains, vectors, and media. The *S. cerevisiae* strains used in this study were isogenic to the W303 genetic background. A detailed description of the strains is provided in Table 1. Deletions of the indicated ORFs were performed with a *URA3*MX cassette as described previously (13) and followed by marker elimination through culturing on 5-fluoroorotic acid (5-FOA) plates. All deletions were confirmed by PCR. The pRS415-OMA1-6×His-Myc, pRS415-OMA1-6×His-Myc H203A (13), pADH1-Msn2-GFP (17), and pCUP1-6×Myc-Cki1 (2–200) (18) plasmids were used to transform the indicated strains.

Cells were cultured in standard yeast extract-peptone (YP) or synthetic complete (SC) medium supplemented with appropriate nutrients and either 2% glucose, 2% galactose, or 2% glycerol-lactate as a sole carbon source.

Construction of a *C. albicans oma1*Δ/Δ mutant. *C. albicans* strain SC5314 (a clinical isolate from the blood; clade 1) (19) was used to generate the *oma1*Δ/Δ mutant by utilizing a *NAT1-Clox* deletion cassette

Downloaded from http://mcb.asm.org/ on September 9, 2016 by University of Aberdeen

developed by Shahana et al. (20). The mutant was obtained in two subsequent transformation rounds. First, an *oma1*::*NAT1-Clox* cassette was PCR amplified from the plasmid pLNMCL (20) with 92-bp flanking homology to the 5′ upstream region and 96-bp flanking homology to the 3′ downstream region of the *OMA1* gene (primers OMA1_NAT1_F1, 5′-ATTTATCCTGGAATGTTCACCAGCCCCCCCTTTAAACTTGCCTACAGTTGACCAATAACATTAGTCGAGGCAGATCAGTGGAAAAATATTATTACGGCCAGTGAATTGTAATA-3′, and OMA1_NAT1_R1, 5′-TTGTTAGTCGATGTAAATGTAATACAAAATGTTTGGTGGTGCTGGTAGTATAGGTGATGGTATTTCACCAATGGTATGGCCACCAACACACCTTAGATCGGAATTAACCCTCACTAA-3′). The transformants with one inactivated allele were selected on nourseothricin (Nou)-containing rich medium with 2.5 mM methionine and 2.5 mM cysteine. The genotypes of heterozygous mutants were confirmed by diagnostic PCR. Single colonies were then restreaked on yeast extract-peptone-dextrose (YPD) medium without supplementation to resolve the *oma1*::*NAT1-Clox* cassette. The further selected Nou-susceptible (Nou^s) isolates were used for the next round of transformation with the PCR-amplified *oma1*::*NAT1-Clox* cassette (primers OMA1_NAT1_F2, 5′-TCTCTGGGTTTCTATCACAACTTTTTTTTCTCTCTGGTTTCGAGTGGAGCATGGAAAATGAATTTGCATTAGGGAAATAACAAGAGTAATAACCCAAATACGGCCAGTGAATTGTAATA-3′, and OMA1_NAT1_R2, 5′-GTGAGAGCCAAGAGGTAACAAAGAATAATCTATATTGAATATTTAACTCTAAGCACAATGGTATAAAACTTCAAGTCTTGGTACCATGTACAAATCGGAATTAACCCTCACTAA-3′). The selected Nou-resistant (Nou^r) mutants were analyzed by PCR to confirm the disruption of both *OMA1* alleles.

Growth conditions. Yeast cells were synchronized as described previously (21). Quantitative assessment of a strain's survival under stress was done through determination of CFU as described previously (13). Cultures were grown to an A_{600} of 0.5 and treated with either 0.5 or 1 mM H_2O_2 for 1 h. The cells were then plated on YP-glucose plates to determine their ability to form viable colonies. Yeast cells for fluorescence microscopy were grown in synthetic selective medium and treated as described above.

Fluorescence techniques. For fluorescence microscopy, synchronized live cells were visualized using the Olympus IX81-FV5000 confocal laser scanning microscope at 488- or 543-nm laser lines with a 100× oil lens. Images were acquired and processed with Fluoview 500 software (Olympus America). Fluoresence-activated cell sorter (FACS) analyses were performed as described previously (15). The oxygen radicals generated by cells at various growth stages were quantitated using the fluorescent dyes dehydroethidium (DHE) (Life Sciences), MitoSox (Life Sciences), and dihydrorhodamine 123 (DHR123) (Cayman Chemical).

Killing of *C. albicans* strains by neutrophils. Polymorphonuclear neutrophils (PMNs) were isolated from peripheral blood of healthy donors by gradient density centrifugation in Histopaque 1077 and Histopaque 1119 (Sigma) as described previously (22). The isolated PMNs were resuspended in RPMI 1640 medium with fetal bovine serum (FBS) (Life Technologies) at a concentration of 10^7 cells/ml. Neutrophil killing was assayed as described previously (23), with minor modifications. Briefly, the *C. albicans* cells were collected in mid-logarithmic phase by centrifugation at 4,000 × *g* for 5 min, counted, and resuspended in sterile phosphate-buffered saline (PBS) at a concentration of 10^6 cells per ml. *C. albicans* cells (200 μl) were incubated with 200 μl of PMNs at a final ratio of 1:10 and 200 μl of RPMI medium. The cultures were incubated for 2 h at 37°C under 5% CO_2. The PMNs were lysed by addition of 100 μl of 0.25% SDS and a short incubation at 30°C for 5 to 10 min. Ice-cold water (900 μl) was added and vigorously mixed, and the mixture was incubated with 50 U of DNase 1 in 100 μl 10× PBS for 15 min at 30°C; 100 μl of the mixture was plated on YPD agar, and CFU were counted after 48 h at 30°C.

***G. mellonella* killing assay.** Virulence assays were performed in the *Galleria mellonella* larva infection model. Animals were injected with 6×10^4 *C. albicans* cells in 10 μl of PBS or with PBS alone in the last proleg. The larvae were maintained at 37°C, and viability was assessed twice daily.

Quantitative real-time PCR. Total RNA was prepared with an RNA purification kit (Epicentre) by following the manufacturer's instructions. cDNA was prepared using a cDNA synthesis kit (Bio-Rad). Quantitative real-time PCR was performed on a Bio-Rad iCycler using Sybr green master mix (Bio-Rad). All samples were examined in triplicate, and the values were normalized to the expression of β-actin. The values were calculated using the $\Delta\Delta C_T$ method. Statistical significance was determined using the threshold cycle (C_T) value.

Miscellaneous biochemical assays. Catalase enzymatic activity was determined as described previously (24). The activity was normalized to total protein in the sample and is presented as micromoles of decomposed hydrogen peroxide per minute and milligram of protein.

Whole-cell trichloroacetic acid (TCA) extracts were generated as previously described (15). The extracts were separated by SDS-PAGE and transferred onto nitrocellulose. All the gels were run under the same experimental conditions. Immobilized polypeptides were incubated with the indicated primary antibodies and horseradish peroxidase-conjugated secondary antibodies and visualized with chemiluminescent substrates (Thermo Scientific). Antiporin, antihemagglutinin (anti-HA), anti-Kar2, anti-green fluorescent protein (anti-GFP), and anti-Pgk1 antibodies were obtained from Life Technologies, Santa Cruz Biotechnology, Abcam, and Sigma. Images were scanned and cropped to prepare the figures, with cropping lines indicated. The intensities of the bands were quantified using ImageJ software (http://rsb.info.nih.gov/ij/).

Statistical analyses. Statistical analyses were conducted using Microsoft Excel. At least three independent replicates were obtained for each experiment presented. Unless otherwise specified, the results were analyzed using one-way analysis of variance (ANOVA) or an unpaired *t* test. *P* values of <0.05 were considered statistically significant.

RESULTS

Oma1-deficient cells are resistant to rapamycin and exhibit reduced TOR signaling. Oma1 activation in the mitochondria occurs under various stress conditions, but beyond this, much remains to be learned regarding its role in stress tolerance. To better understand the role of Oma1 in mitochondrial stress tolerance, we conducted a miniscreen aiming to test the fitness responses of the Oma1-deficient mutant to 25 varied chemical compounds known to impact the growth of yeast cells (Table 2). Our screen revealed that, unlike wild-type (WT) cells, *oma1*Δ cells showed enhanced resistance to compounds linked to TOR signaling, including caffeine and vanillin (25, 26) (Fig. 1A) and, most notably, the TOR pathway-inactivating antibiotic rapamycin (Fig. 1A and 2A). This effect is specific to Oma1 deficit, as loss of the other IM-bound proteases, Pcp1 and Yme1 (*i*-AAA), or *m*-AAA (via deletion of its Yta10 subunit) did not produce increased rapamycin tolerance (Fig. 2A and data not shown). Moreover, the *oma1*-null allele is dominant in the *yme1*Δ background but not in the *yta10*Δ background, as an *oma1*Δ *yme1*Δ double-deletion strain was also mildly resistant to rapamycin. Importantly, lack of resistance to the antibiotic oligomycin (Fig. 1B) and unaltered expression of the key multidrug resistance proteins Pdr5 and Pdr15 (Fig. 1C) indicate that the enhanced rapamycin tolerance of the *oma1*Δ strain is not due to the activated multidrug resistance pathway. Collectively, these observations suggest that loss of Oma1 likely exerts a negative effect on TOR signaling (27, 28).

The TOR complex 1 (TORC1) effector kinase Npr1, which exists in both hyperphosphorylated and dephosphorylated forms, exhibits a specific separation pattern on SDS-PAGE, with the former form migrating slower than the latter form (29). Published data indicate that the hyperphosphorylated state is significantly

Downloaded from http://mcb.asm.org/ on September 9, 2016 by University of Aberdeen

TABLE 2 Sensitivity of *oma1*Δ cells to various stressors

Compound or chemical	Concn tested	Response (relative to WT control)
NaCl	1 M	No difference
Sorbitol	0.8 M	No difference
$CaCl_2$	100 mM	No difference
$CuCl_2$	2 mM	No difference
$CdCl_2$	2 mM	No difference
$NaAsO_2$	1 mM	No difference
Buthionine sulfoximine (BSO)	5 mM	No difference
Dithiothreitol (DTT)	4 mM	No difference
Cycloheximide	1 μg/ml	No difference
Tunicamycin	1 μg/ml	No difference
Canavanine	10 μg/ml	No difference
Phenylmethylsulfonyl fluoride (PMSF)	4 mM	No difference
2-Deoxyglucose (2-DG)	0.1%	No difference
Dibutyryl cyclic AMP (dbcAMP)	1 mM	No difference
Rapamycin	30 ng/ml	Resistant
Myriocin	25 μg/ml	No difference
Caffeine	15 mM	Resistant
Vanillin	10 mM	Resistant
Concanamycin A	5 μM	No difference
Caspofungin	0.1 μg/ml	Sensitive
Iodoacetamide	30 μM	No difference
Antimycin A	5 μM	No difference
EDTA	5 mM	No difference
Oligomycin	10 μg/ml	No difference

decreased in *tor1*Δ cells (29, 30). Therefore, to further corroborate reduced TOR signaling in the *oma1*Δ mutant, we chromosomally tagged Npr1 with a 3×HA epitope tag in WT, *oma1*Δ, and *tor1*Δ cells and monitored its electrophoretic behavior by immunoblotting. We reproducibly observed a significant decrease in the abundance of hyperphosphorylated Npr1 in *tor1*Δ cells, as well as in WT cells treated with rapamycin (Fig. 2B and C). Importantly, the basal levels of phosphorylated Npr1 were significantly lower in *oma1*Δ cells than in the WT (Fig. 2B and C), reflecting decreased basal TORC1 activity. The expression levels of Tor1 and Tor2 (components of the TORC1 and TORC2 complexes, respectively) were comparable between the *oma1*Δ strain and the wild-type control (Fig. 2D). Altogether, our data suggest that certain aspects of TORC1-related signaling are impeded in *oma1*Δ cells.

Loss of Oma1 impinges on the TORC1-Rim15-Msn2/Msn4 signaling axis. Loss of Oma1 may lead to elevated mitochondrial ROS production during active growth, which acts as an adaptation signal that impinges on the conserved TORC1 pathway (11). Several signaling cascades intersect with TORC1 or converge on its downstream targets (4, 31). To determine which facet of TOR signaling is impeded by Oma1 loss-associated ROS emission, we examined genetic interactions of *OMA1* and genes encoding key components of TORC1-related pathways (Fig. 3A). Deletion of *OMA1* in Sch9 kinase-deficient cells improved the growth of the mutant on rapamycin-containing plates (Fig. 3B, row 4), indicating the dominant nature of the *oma1*-null allele in the *sch9*Δ background. Deletions of *OMA1* in combination with genes encoding retrograde pathway components (the transcription factor Rtg1 or its sensor, Rtg2) did not significantly influence the rapamycin phenotype of the cells in question (Fig. 3B, row 6, and data not shown), probably because the *rtg1*Δ mutant alone also exhibited resistance to the drug (Fig. 3B, line 5). Similarly, reduction of cyclic AMP (cAMP)-protein kinase A (PKA) signaling through deletion of the adenylate cyclase activator Ras2 (Fig. 3B, row 12) or enhancement of PKA activity via disruption of the cAMP phosphodiesterase Pde2 (Fig. 3B, row 14) did not influence the rapamycin resistance of *oma1*Δ cells. In contrast, the rapamycin resistance of *oma1*Δ cells was abolished by deleting either Tor1 or its downstream target, the PAS kinase Rim15 (Fig. 3B, rows 8 and 10), mimicking single deletions of these genes (32). Inactivation of Avo2, a nonessential subunit of the rapamycin-insensitive complex TORC2 (33), did not affect the rapamycin resistance of the *oma1*Δ strain (Fig. 3C), indicating that loss of Oma1 primarily reduces signaling via the Tor1-containing complex. In line with these observations, TORC1 appears to be a limiting factor in the *oma1*Δ-mediated epistatic effects, as loss of *TOR1* ablated the rapamycin-resistant phenotype of the *sch9*Δ *oma1*Δ cells (Fig. 3D). We thus conclude that modules of the TORC1-Rim15 signaling axis are located downstream of *OMA1*.

Because the TORC1-Rim15 axis is known to control certain aspects of pancellular stress responses (4), we examined the oxidative-stress resistance of the above-mentioned strains by testing their ability to form viable colonies following treatment with 1 mM H_2O_2 in log phase. As reported previously (13), *oma1*Δ cells were sensitive to H_2O_2. Consistent with the dominant nature of the *oma1*-null allele in the *sch9*Δ background, loss of *SCH9* did not significantly improve the sensitivity of *oma1*Δ cells to H_2O_2. On the other hand, deletion of *TOR1* or *RIM15* in the *oma1*Δ background conferred H_2O_2 resistance (Fig. 3E), which was markedly increased for *tor1*Δ *oma1*Δ cells relative to the WT control. Loss of *TOR1* even enhanced the H_2O_2 resistance of the *sch9*Δ *oma1*Δ strain (data not shown), further indicating that sensitization of *oma1*Δ cells to oxidants occurs via TORC1 signaling. Interestingly, *tor1*Δ *oma1*Δ cells also exhibited a slight, but statistically significant, increase in H_2O_2 survival relative to the *tor1*Δ mutant, suggesting that the relationship between Oma1 and TORC1 may be more complex and involve additional factors.

In *S. cerevisiae*, the TORC1-Rim15 axis orchestrates several transcription factors, including Gis1 and Msn2/Msn4 (4, 10). While the above-described results suggest that the Msn2/Msn4-mediated oxidative-stress response is altered in *oma1*Δ cells, it is possible that Gis1 is also involved. To distinguish between these scenarios, we analyzed the sensitivity of *oma1*Δ *gis1*Δ and *oma1*Δ *msn2*Δ *msn4*Δ cells to rapamycin. The loss of Gis1 (Fig. 3F, rows 9 and 10), Msn2 (Fig. 3F, rows 3 and 4), or Msn4 (Fig. 3F, rows 5 and 6) in the *oma1*Δ background had no appreciable effect on drug resistance. Conversely, the disruption of Msn2 and Msn4 in *oma1*Δ cells abolished rapamycin resistance (Fig. 3F, row 8). Moreover, the *oma1*Δ *msn2*Δ *msn4*Δ cells showed improved H_2O_2 survival relative to the *oma1*Δ mutant alone (Fig. 3G). These data indicate that deregulation of TORC1-Rim15-Msn2/Msn4 signaling is a likely contributor to several phenotypes seen in the *oma1*Δ strain, including rapamycin resistance and oxidative-stress sensitivity.

Oxidative-stress signaling is compromised in *oma1*Δ cells. To better understand the reduced tolerance of Oma1-deficient cells for oxidative stress, we monitored the expression of the two Msn2/Msn4-controlled oxidative-stress-responsive genes: catalase (*CTT1*) and manganese superoxide dismutase (*SOD2*). Whereas expression of these genes was greatly upregulated in WT cells treated with 0.5 mM H_2O_2, as reported previously (34), their expression was largely unchanged in peroxide-treated *oma1*Δ cells

Downloaded from http://mcb.asm.org/ on September 9, 2016 by University of Aberdeen

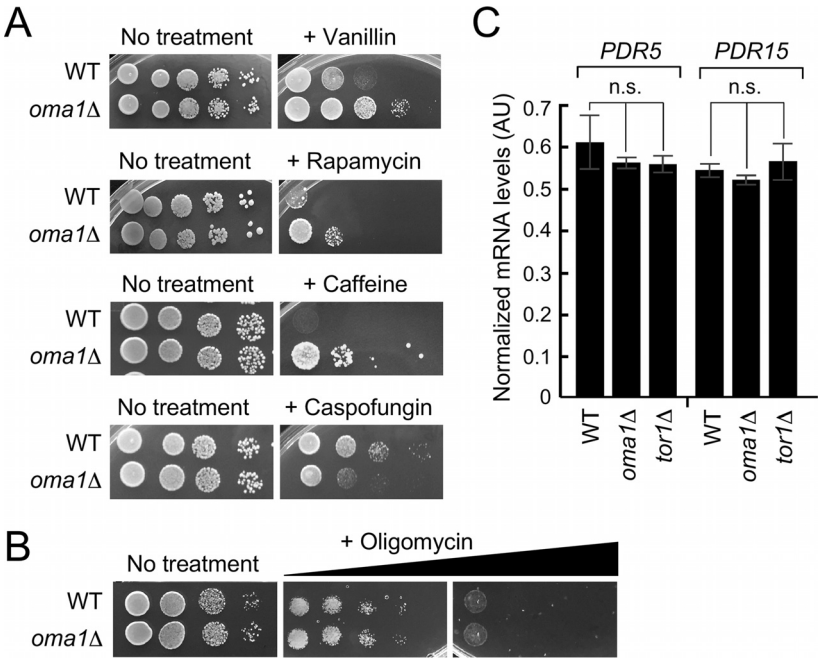

FIG 1 Tolerance of the *oma1*Δ mutant for selected chemical compounds. (A) Growth of WT and *oma1*Δ cells on plates with or without 10 mM vanillin, 30 ng/ml rapamycin, 15 mM caffeine, and 0.1 μg/ml caspofungin. Synchronized cells were grown to mid-logarithmic stage (8 h of growth; $A_{600} = 0.8$), serially diluted, and spotted onto the respective plates. Photographs were taken after 2 (No treatment) or 4 (plus compound) days at 28°C. (B) Growth of WT and *oma1*Δ strains on plates containing increasing concentrations of oligomycin. The cells were handled as in panel A and spotted onto plates containing 10 μg/ml or 250 μg/ml oligomycin. Photographs were taken after 2 days of incubation at 28°C. (C) Relative expression of *PDR5* and *PDR15* in the indicated strains. The error bars indicate standard deviations (SD) ($n = 4$ biological replicates); n.s., nonsignificant by Student's *t* test. AU, arbitrary units.

(Fig. 4A). Furthermore, attenuated *CTT1* transcript levels in the *oma1*Δ mutant were reflected by reduced catalase activity following H_2O_2 exposure (Fig. 4B). No significant difference in basal catalase levels between WT and *oma1*Δ cells was observed.

Given that Msn2/Msn4 accumulate in the nucleus upon H_2O_2 treatment (35), we wanted to test if localization is altered in *oma1*Δ cells upon cellular stress. Using confocal microscopy (CFM), we examined the nuclear accumulation of GFP-tagged Msn2 in glucose-grown cells exposed to 1 mM H_2O_2. Compared with the WT control, *oma1*Δ cells accumulated significantly more

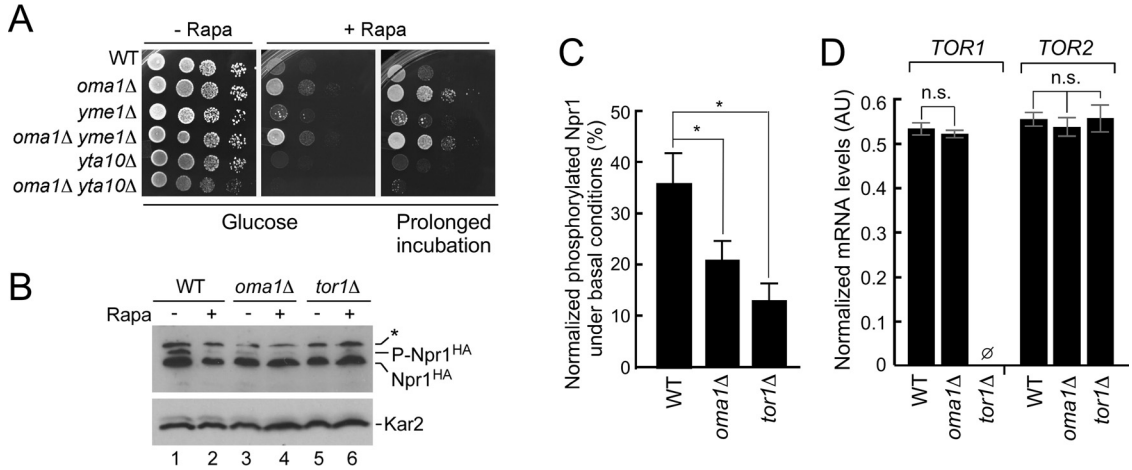

FIG 2 Oma1-deficient cells are resistant to rapamycin and exhibit attenuated TOR activity. (A) Growth of the indicated strains on YPD plates with (+Rapa) or without (−Rapa) 30 ng/ml rapamycin. Synchronized cells were grown to mid-log stage (8 h of growth; $A_{600} = 0.8$). Photographs were taken after 2 (−Rapa), 4 (+Rapa), or 6 (+Rapa, Prolonged incubation) days at 28°C. (B) WT, *oma1*Δ, and *tor1*Δ strains expressing genomically tagged Npr1-HA were cultured in the presence or absence of rapamycin. Log-phase cells were harvested, lysed, and analyzed by immunoblotting with antibodies against HA epitope and Kar2 (loading control). $Npr1^{HA}$ and P-$Npr1^{HA}$, dephosphorylated and hyperphosphorylated forms of the protein, respectively. The asterisk indicates an HA tag-cross-reacting band. (C) Quantitation of the P-Npr1-HA form in WT, *oma1*Δ, and *tor1*Δ cells. The error bars indicate standard errors of the mean (SEM) ($n = 3$ biological replicates). (D) Relative expression of *TOR1* and *TOR2* in the indicated strains. The error bars indicate SD ($n = 4$ biological replicates). *P* values were determined as for Fig. 1 (n.s., nonsignificant; *, $P < 0.05$ by Student's *t* test). Ø, no detectable signal.

Downloaded from http://mcb.asm.org/ on September 9, 2016 by University of Aberdeen

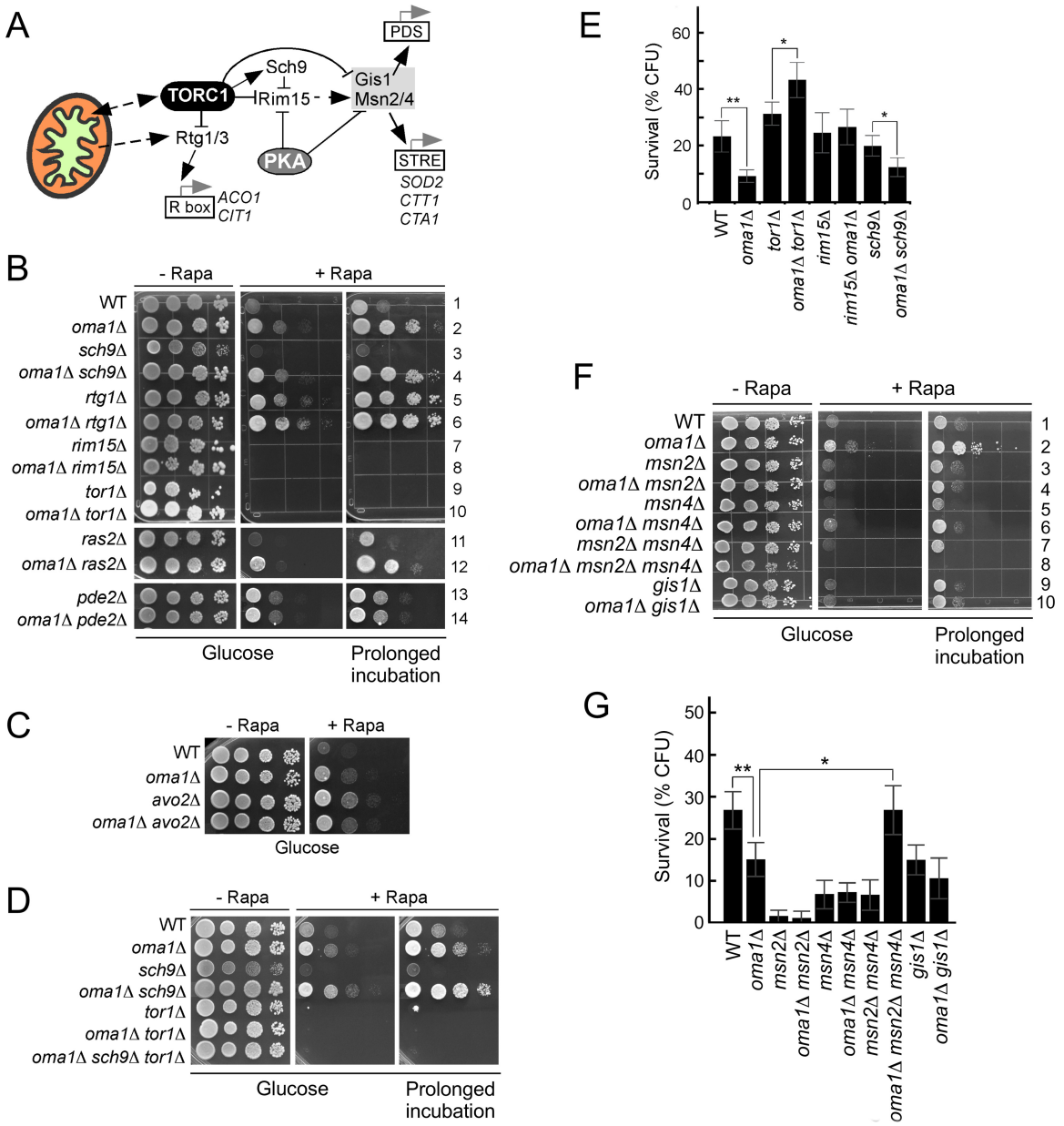

FIG 3 The TORC1-Rim15-Msn2/Msn4 signaling axis is downstream of *OMA1*. (A) Model demonstrating key components of mitochondrion-related signaling in yeast. (B to D) Growth of the indicated strains on YPD plates with or without rapamycin (30 ng/ml). Cells were analyzed as for Fig. 1. (E) Oxidative-stress survival of the indicated strains. Log-phase cultures (8 h; $A_{600} = 0.5$) were acutely treated with 1 mM H_2O_2 for 1 h. Samples were diluted to 300 cells and plated for survival on YPD plates. The number of CFU was determined after 2 days at 28°C. The bars show means and SD ($n = 5$). *, $P < 0.05$; **, $P < 0.01$ by Student's *t* test and one-way ANOVA. (F) Growth of indicated strains on YPD and YPD-plus-Rapa plates. (G) H_2O_2 stress survival of the indicated strains.

Msn2-GFP in the nucleus upon peroxide treatment (Fig. 4C and D). Importantly, Msn2-GFP steady-state levels were not altered by the *oma1*Δ mutation (Fig. 4E). Similar results were obtained when 0.1 mM or 0.5 mM H_2O_2 was used (Fig. 4F and G). To test the specificity of this response, we examined Msn2-GFP localization in response to a hyperosmotic insult. Unlike with H_2O_2 stress, wild-type and *oma1*Δ cells showed similar levels of nuclear Msn2-GFP accumulation upon exposure to 1 M NaCl (Fig. 4H and I). This is consistent with the finding that Oma1-deficient cells show no sensitivity to NaCl. The more robust nuclear localization of Msn2-GFP in response to NaCl treatment (relative to H_2O_2 treatment) is likely due to the fact that Msn2/Msn4-mediated core (environmental) stress responses are better "tuned" toward more natural environmental stressors, such as osmotic shock. Taken together, these data led us to conclude that Msn2/Msn4-mediated oxidative-stress signaling is specifically compromised by Oma1 inactivation.

The TORC1 effector PP2A phosphatase contributes to abnormal Msn2 activity and impaired H_2O_2 tolerance in the *oma1*Δ mutant. Despite the enhanced oxidative-stress-induced nuclear localization of Msn2, its function appears to be impeded in the *oma1*Δ mutant. A recent report implicated protein phos-

Downloaded from http://mcb.asm.org/ on September 9, 2016 by University of Aberdeen

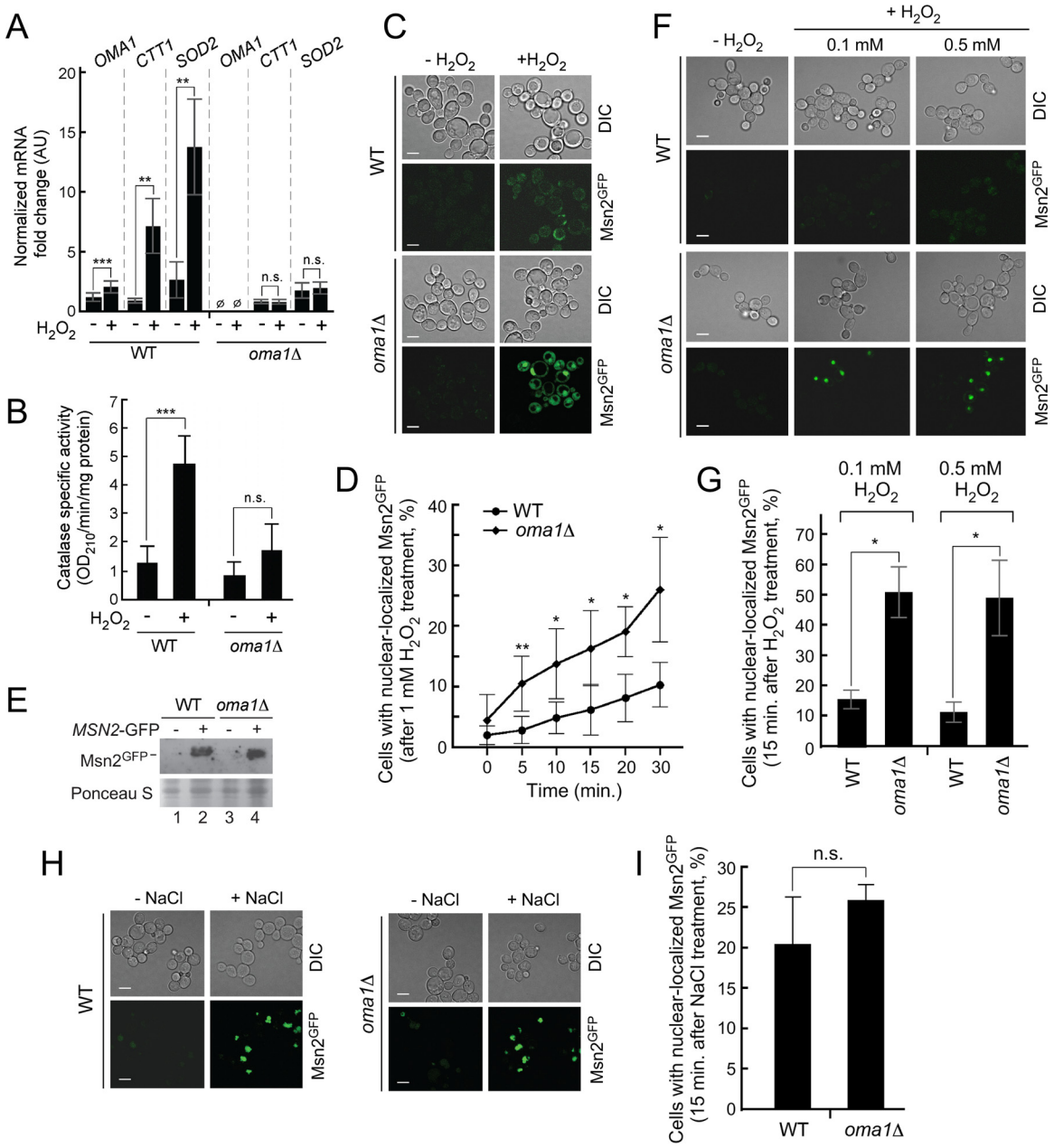

FIG 4 Oxidative- but not osmotic-stress response mediated via the Msn2/Msn4 signaling node is altered in *oma1*Δ cells. (A) Transcript changes in synchronized WT and *oma1*Δ cells in response to acute treatment with 0.5 mM H_2O_2. Relative transcript levels of *OMA1*, cytosolic catalase (*CTT1*), and manganese superoxide dismutase (*SOD2*) were assessed by quantitative PCR (qPCR) ($n = 5$ independent experiments). (B) Catalase activity in whole-cell extracts derived from the indicated cells ($n = 3$ biological replicates). The bars show mean values and SD. (C and D) Nuclear accumulation of Msn2-GFP in 1 mM H_2O_2-exposed WT and *oma1*Δ cells. (C) Representative images showing Msn2-GFP localization at 15 min posttreatment. (D) Quantitation of time-dependent nuclear accumulation of Msn2-GFP. The error bars indicate SD ($n = 3$, with 800 cells per biological replicate). (E) Steady-state levels of Msn2-GFP in WT and *oma1*Δ cell lysates. Proteins were visualized with antibodies against the GFP moiety. (F and G) Nuclear accumulation of Msn2-GFP in 0.1 or 0.5 mM H_2O_2-exposed WT and *oma1*Δ cells. (F) Representative images showing Msn2-GFP localization at 15 min posttreatment. (G) Quantitation of nucleus-localized Msn2-GFP. The error bars indicate SD ($n = 3$, with 800 cells per biological replicate). (H and I) Nuclear accumulation of Msn2-GFP in response to 1 M NaCl was analyzed as for panels C, F, and G. n.s., nonsignificant; *, $P < 0.05$; **, $P < 0.01$; ***, $P < 0.001$ by Student's *t* test.

phatase 2A (PP2A) in facilitating Msn2/Msn4 association with chromatin via modulation of nuclear sequestration mechanisms in response to signals from TORC1 (17). Moreover, alterations in TORC1 cues can attenuate the transcriptional activity of Msn2/Msn4 via several factors, including PP2A phosphatase (36). That is, response to H_2O_2 treatment requires not only nuclear translocation of the Msn2/Msn4 complex but also its activation via PP2A-mediated mechanisms (Fig. 5A). Therefore, we sought to test if loss of the catalytic subunits of PP2A, Pph21 and Pph22, would affect the rapamycin resistance of the *oma1*Δ strain. Deleting *PPH21* or *PPH22* only slightly attenuated the phenotype of *oma1*Δ cells. However, the *oma1*Δ *pph21*Δ *pph22*Δ triple mutant

Downloaded from http://mcb.asm.org/ on September 9, 2016 by University of Aberdeen

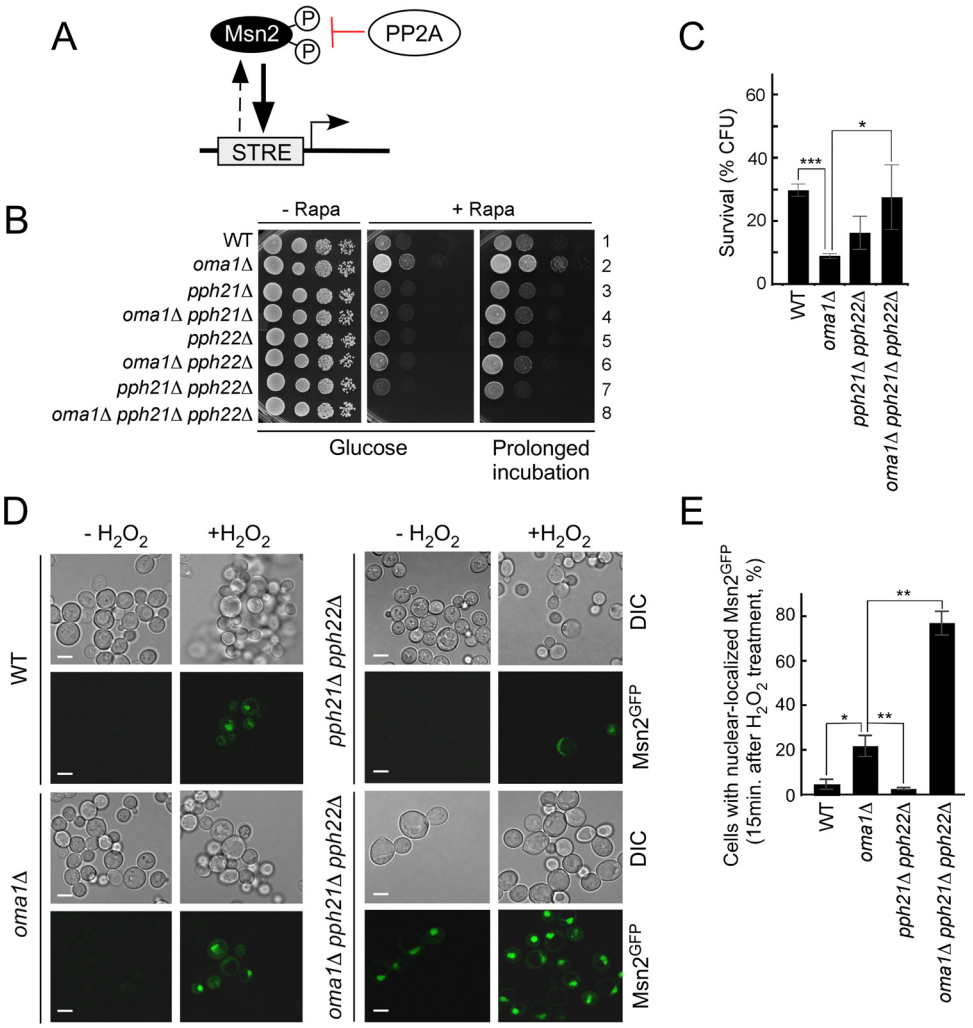

FIG 5 Mitochondrial function, ROS production, and antioxidant defense in the *oma1*Δ strain. (A) Schematic showing the relationship between the PP2A phosphatase and the transcriptional factor Msn2. (B) Growth of the indicated strains on YPD plates with or without rapamycin (30 ng/ml). (C) Oxidative-stress survival of the indicated strains determined as described for Fig. 3E. (D and E) Nuclear accumulation of Msn2-GFP in the indicated strains at 15 min after treatment with 1 mM H_2O_2. (D) Representative confocal microscopy images. (E) Quantitation of nucleus-localized Msn2-GFP. Cells were handled and analyzed as described for Fig. 3D. *, $P < 0.05$; **, $P < 0.01$; ***, $P < 0.001$ by Student's *t* test.

was very sensitive to this TORC1 inhibitor (Fig. 5B, row 8), reflecting the importance of PP2A in the rapamycin resistance of Oma1-deficient cells. Moreover, combined loss of *PPH21* and *PPH22* in *oma1*Δ cells restored their tolerance for acute H_2O_2 stress (Fig. 5C).

Deletion of the PP2A subunits in the *oma1*Δ strain resulted in even higher nuclear accumulation of Msn2-GFP reporter than in the control strains (Fig. 5D and E). These observations are consistent with the idea that PP2A functions downstream of the events leading to nuclear accumulation of Msn2/Msn4. These data indicate that the PP2A phosphatase modulates Msn2/Msn4 activity and oxidative-stress sensitivity in the *oma1*Δ strain.

Transiently elevated ROS production contributes to reduced TOR signaling in Oma1-deficient cells. Mitochondria generate cues that regulate a number of cellular processes, including oxidative-stress tolerance (11, 37–40). Mitochondrion-emitted ROS appear to be central to many of these events (6). We recently demonstrated that loss of Oma1 leads to unbalanced respiration and enhanced ROS production (41). To further explore this observation, we stained synchronized WT and *oma1*Δ cells at various growth stages with the superoxide ($O_2^{\cdot-}$)-sensitive dye DHE and monitored their fluorescence by flow cytometry. Consistent with previous reports (11), we observed low basal levels of DHE fluorescence in exponentially growing WT cells. We also confirmed the increase in endogenous $O_2^{\cdot-}$ production in stationary-phase cells. However, we found that during log phase, *oma1*Δ cells reproducibly accumulate relatively high levels of $O_2^{\cdot-}$ (Fig. 6A). The superoxide levels were comparable in diauxic *oma1*Δ and WT cells (data not shown), indicating that ROS levels in WT cells eventually catch up to those in the *oma1*Δ mutant. We therefore tested ROS levels in stationary phase and found that the DHE staining in the *oma1*Δ mutant was comparable to that in the WT (Fig. 6A). Similar results were obtained with the $O_2^{\cdot-}$-specific dye MitoSox (not shown) and with the H_2O_2-specific dye dihydrorhodamine 123 (Fig. 6B). Because the temporal increase in ROS and elevated oxygen consumption in exponential-phase *oma1*Δ cells

Downloaded from http://mcb.asm.org/ on September 9, 2016 by University of Aberdeen

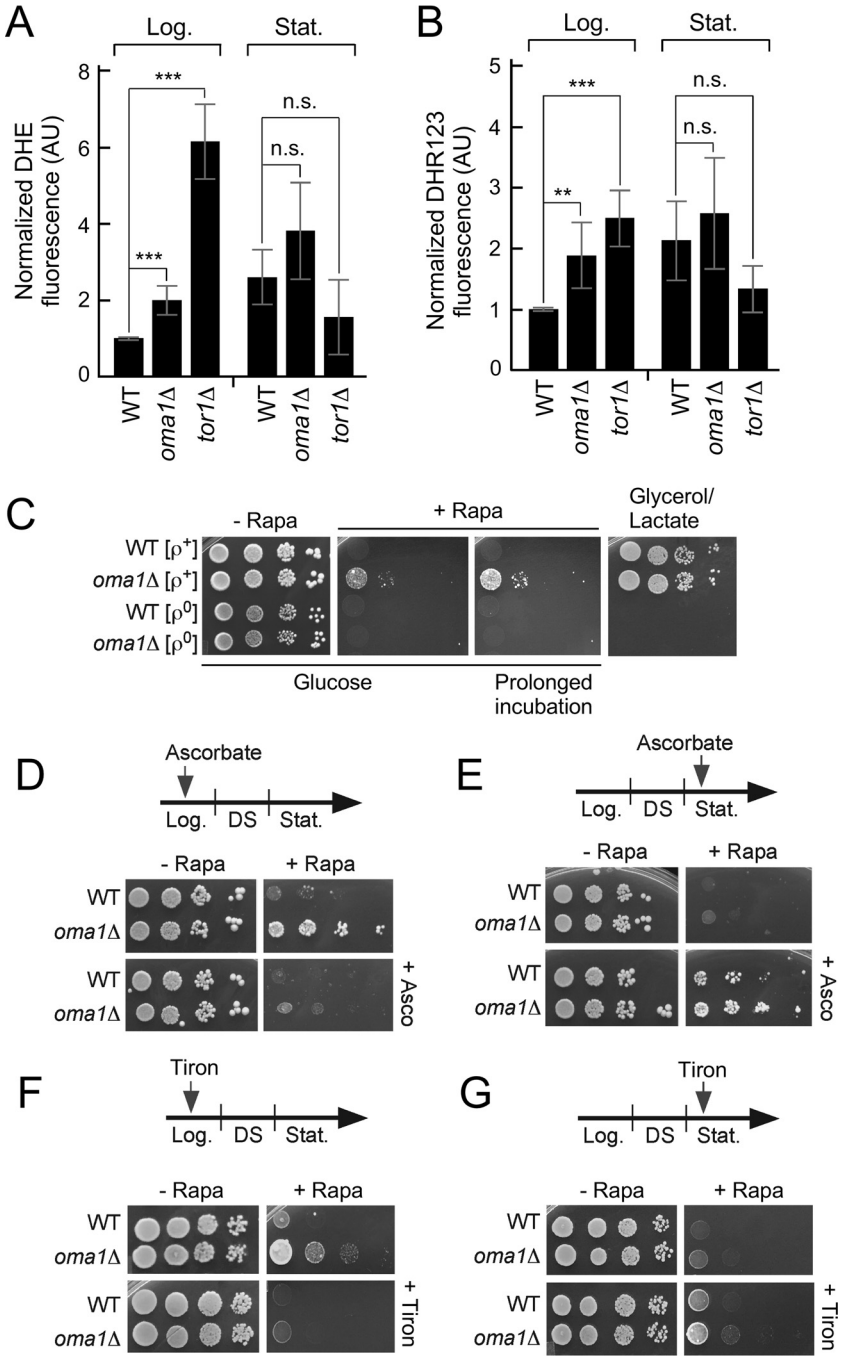

FIG 6 Transiently elevated ROS contribute to rapamycin resistance of the *oma1*Δ mutant. (A and B) ROS production determined by FACS analysis of synchronized DHE-stained (A) or DHR123-stained (B) WT and *oma1*Δ cells at log (Log.) (A_{600} = 0.5 6 h postinoculation) and stationary (Stat.) (A_{600} = 3.0 12 h postinoculation) stages. The data show mean values and SD (n = 3 to 5 biological repeats). (C) Growth of the indicated strains with (ρ^+) or without (ρ^0) mtDNA. (D to G) Growth of antioxidant-pretreated WT and *oma1*Δ strains. Synchronized exponential-phase cells (8 h of growth; A_{600} = 0.8) cultured with or without 5 μM sodium ascorbate (D) or 20 mM the ROS scavenger Tiron (F) were analyzed as described above. (E and G) Ascorbate pretreatment (E) and Tiron pretreatment (G) showing growth of the same strains analyzed in stationary phase (24 h of growth; A_{600} = 8.0). n.s., nonsignificant; **, $P < 0.01$; ***, $P < 0.001$ by Student's t test.

partially phenocopy mutants with reduced TOR signaling (11) (Fig. 6A and B), we hypothesized that reduced TORC1 activity in *oma1*Δ cells may be a consequence of transiently elevated intracellular ROS.

To examine the link between elevated radicals in log-phase *oma1*Δ cells and deregulated TOR signaling, we tested whether preventing ROS accumulation in these cells ameliorates the rapamycin resistance of the strain. Electron transport chain (ETC) complexes are one of the primary sources of ROS in a cell (6). Thus, we compared the rapamycin growth phenotypes of *oma1*Δ strains with ([*rho*$^+$]) and without ([*rho*^{0}]) the mitochondrial ge-

Downloaded from http://mcb.asm.org/ on September 9, 2016 by University of Aberdeen

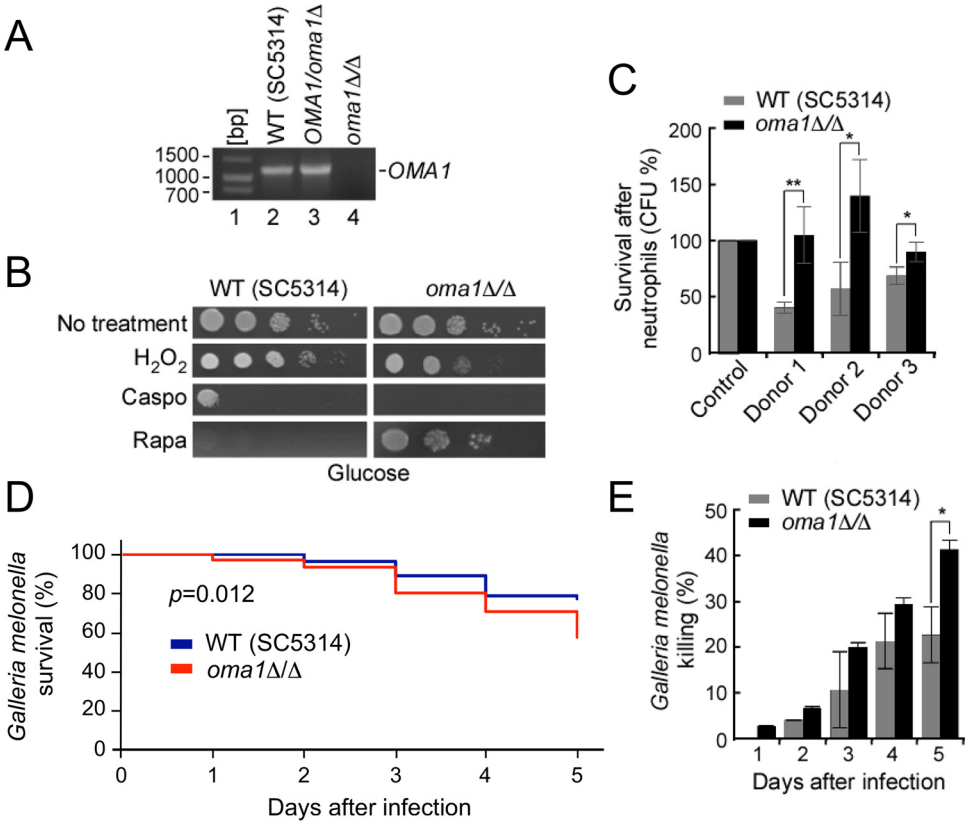

FIG 7 Loss of Oma1 impinges on TOR signaling and promotes virulence in *C. albicans*. (A) PCR confirming homozygous deletion of *orf19.3827/OMA1* in *C. albicans* strain SC5314. (B) Sensitivity of the SC5314 and *oma1*Δ/Δ strains to various stressors. Mid-log-stage cells were grown on YPD plates containing 5 mM H_2O_2, 0.1 μg/ml caspofungin (Caspo), or 0.4 μg/ml rapamycin (Rapa). The plates were placed in the 30°C static incubator, and photographs were taken 24 h after spotting. (C) Survival of *C. albicans* strains in human neutrophils. The indicated strains (1×10^6 cells) were isolated, washed, and cocultured with 1×10^7 RPMI medium-plus-FBS-treated polymorphonuclear granulocytes from 3 unrelated healthy donors. Following 2-h coincubation at 37°C, pathogen cells were reisolated and plated for survival. The viable colonies were assessed after 48 h at 30°C. (D and E) Survival of *G. mellonella* larvae infected with the indicated strains. The larvae were injected with cells or buffer and monitored for 5 days at 37°C. $n = 25$ subjects per replicate for each group plus 10 noninjected animals (nonmanipulated control). Three biological replicates of each experiment were conducted, and two independent isolates of the *oma1*Δ/Δ strain were tested. (D) Kaplan-Meier survival plot of animals infected with the indicated strains (the results show the data pooled for a single comparison; $n = 75$ for each strain). *P* values were determined using log rank statistics. (E) Complementary data showing the percentage of *G. mellonella* killing ± SEM; *P* values were determined as for Fig. 1. *, $P < 0.05$; **, $P < 0.01$ by Student's *t* test.

nome. Loss of mitochondrial DNA (mtDNA) (encoding several key ETC subunits) completely abrogated the rapamycin resistance of the *oma1*Δ mutant (Fig. 6C). Moreover, pretreatment of log-phase *oma1*Δ cells ($A_{600} = 0.5$) with the ROS scavenger ascorbate (Fig. 6D) or the antioxidant Tiron (Fig. 6F) negated their ability to grow on rapamycin-containing plates. In line with the idea of hormetic-like ROS adaptation in exponential-phase cells (11), postdiauxic *oma1*Δ cells were unable to survive on rapamycin plates (Fig. 6E and G). This is likely due to the fact that stationary-phase *oma1*Δ cells do not exhibit elevated ROS (Fig. 6B); the previously reported progressive decline of respiratory function in these cells may also contribute to the loss of rapamycin resistance. Interestingly, the pretreatment of stationary WT and *oma1*Δ cultures with antioxidants had an advantageous effect on their growth on rapamycin plates, suggesting that dampening ROS in postdiauxic cells may be beneficial for their survival. Collectively, these data indicate that a transient increase in mitochondrial ROS modulates TORC1-related signaling in *oma1*Δ cells.

The Oma1 homolog is necessary for TOR signaling-mediated physiological responses in *C. albicans*. We asked if the impact of Oma1 upon TOR signaling is evolutionarily conserved. To explore this, we examined the role of the Oma1 ortholog in an evolutionarily distant yeast, the human pathogen *C. albicans*. We deleted both alleles of *orf19.3827* (whose products had 45.2% sequence identity to the *S. cerevisiae* Oma1 protein) to construct a homozygous null mutant in the diploid yeast (Fig. 7A). Like the *S. cerevisiae oma1*Δ strain, the *C. albicans oma1*Δ/Δ mutant displayed no obvious phenotype under standard growth conditions. However, consistent with *S. cerevisiae* data, upon stress with 5 mM H_2O_2, *C. albicans oma1*Δ/Δ cells displayed mild growth impairment. Additionally, the survival of the strain was affected by the drug caspofungin (Fig. 7B). Notably, *S. cerevisiae oma1*Δ cells were also found to be caspofungin sensitive in our miniscreen (Fig. 1A). Most significantly, *C. albicans oma1*Δ/Δ cells exhibited marked resistance to rapamycin (Fig. 7B).

TOR pathway components have been implicated as virulence-mediating factors in *C. albicans* (42, 43). We therefore examined the virulence of the *C. albicans oma1*Δ/Δ strain by two independent approaches. First, we tested the survival of WT and *oma1*Δ/Δ cells upon incubation with human PMNs isolated from three dif-

Downloaded from http://mcb.asm.org/ on September 9, 2016 by University of Aberdeen

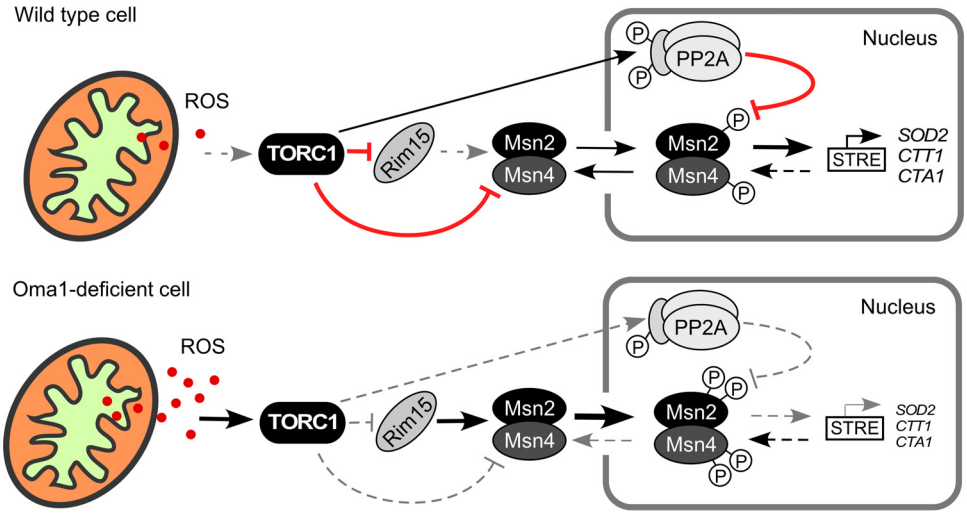

FIG 8 Speculative model of how Oma1 loss affects the TORC1 pathway-dependent oxidative-stress response. Depletion of Oma1 is associated with enhanced production of mitochondrial ROS during exponential growth. Elevated ROS levels exert a modulatory effect on TORC1 signaling, which results in reduced communication via the TORC1-Rim15 axis and reduces activity of the PP2A phosphatase. These alterations lead to improper nuclear transport and/or retention of the Msn2/Msn4 transcriptional complex, thereby reducing the expression of Msn2/Msn4-controlled genes in response to acute oxidative stress. We acknowledge that reduced TORC1 signaling may exert additional effects (not shown in the cartoon) that can also contribute to the reduced oxidative-stress tolerance and rapamycin resistance of *oma1*Δ cells. Black, normal/active signaling; red, inhibited signaling; dashed gray, affected signaling or inhibition.

ferent donors. Surprisingly, the *oma1*Δ/Δ cells exhibited increased resistance to PMN killing (Fig. 7C). This may be due to the higher metabolic plasticity of *C. albicans* and the evolutionary "rewiring" of the TOR pathway at the level of the Msn2/Msn4 node, because, unlike *S. cerevisiae*, these transcription factors do not play a significant role in the pathogen's responses to oxidative stress (44, 45). Next, we tested the virulence of the *oma1*Δ/Δ strain in the established *G. mellonella* larval model of systemic *Candida* infection (46). The larvae injected with rapamycin-resistant *oma1*Δ/Δ cells displayed increased virulence, particularly at day 5 of infection (Fig. 7D and E). Together, our data indicate that, as in *S. cerevisiae*, loss of Oma1 in *C. albicans* impinges on TOR signaling, which impacts on specific physiological properties of the pathogen, including its virulence.

DISCUSSION

Here, we show that loss of the conserved protease Oma1 in yeast reduces signaling via the TORC1-Rim15-Msn2/Msn4 axis, thereby interfering with oxidative-stress responses. These data support a recent model (11, 38, 39) postulating the existence of a transient, adaptive ROS signal necessary for survival in stationary phase in TOR signaling mutants. Our novel finding is the identification of an upstream, mitochondrion-localized, modulator of TOR signaling. Cells lacking Oma1 display (i) elevated resistance to rapamycin, (ii) increased respiration and ROS production during logarithmic growth, and (iii) reduced phosphorylation of the TORC1 effector protein Npr1. These traits are characteristic of strains with reduced TOR activity (11, 28, 29, 47). The loss of the TORC1 subunit Tor1 or its downstream target kinase, Rim15, in *oma1*Δ cells abolishes these traits. Epistatic interactions between *OMA1* and *SCH9* or *RTG1* suggest that these branch point signaling elements are not directly involved. Moreover, Tor1 appears to be a limiting factor in these genetic interactions. The signaling deficit in *oma1*Δ cells is also not due to attenuation of PKA or Ras signaling. Two factors appear to be critical for *oma1*Δ phenotypes. In line with previous reports (11, 37), transient accumulation of ROS in the actively growing *oma1*Δ strain is likely a key contributor to altered TOR signaling. Reducing ROS in logarithmic-phase *oma1*Δ cells with antioxidants, or by genetically blocking respiration, remedies malfunctioning TORC signal transduction. The enhancement in the respiratory capacity of log-phase *oma1*Δ cells likely defines the specificity of the phenotype, because the strains defective in other IM proteases (*yme1*Δ, *yta10*Δ, and *pcp1*Δ) are, to various degrees, respiratory deficient. Consistent with this postulate is the lack of rapamycin resistance in the *oma1*Δ *yta10*Δ mutant, wherein loss of the Yta10 subunit of the *m*-AAA protease results in the complete loss of respiration. It is also noteworthy that the results of our antioxidant pretreatment experiments are in line with the model whereby elevated levels of ROS may be advantageous in younger cells but become detrimental in aged cells (48).

How does suspended TORC1-Rim15 signaling relate to vulnerability of *oma1*Δ cells to stress? Reportedly, alterations in TORC1 cues attenuate the transcriptional activity of Msn2/Msn4 via several factors, including PP2A phosphatase (17, 36). Our study reveals that, despite the enhanced nuclear localization of Msn2 (and presumably Msn4) in response to acute oxidative stress, the expression of Msn2/Msn4-controlled genes is not significantly changed in *oma1*Δ cells. This effect is specific to oxidative insults and appears to underpin the reduced oxidative stress tolerance and rapamycin resistance of *oma1*Δ cells (Fig. 8). Remarkably, inactivation of PP2A alleviates both phenotypes. It is noteworthy that in the W303 genetic background used in this study, oxidation/nuclear retention of another oxidative-stress-responsive redox-sensitive transcriptional factor, Yap1, is largely Hyr1/Gpx3 independent and mediated via the Msn2/Msn4-controlled Srx1-Tsa1 peroxiredoxin relay (49, 50). This situation may therefore potentiate the effect of impaired Msn2/Msn4 function and further contribute to increased sensitivity of *oma1*Δ cells to H_2O_2.

Downloaded from http://mcb.asm.org/ on September 9, 2016 by University of Aberdeen

The association of Oma1 with TOR signaling is not restricted to baker's yeast. Deletion of the *OMA1* ortholog in *C. albicans* results in marked resistance to rapamycin, indicating suspended TOR signaling. However, the modulatory effect of Oma1 loss in *C. albicans* differs from that in *S. cerevisiae*, likely due to higher metabolic plasticity of *C. albicans* and the "rewiring" of interactions between TOR and Msn2/Msn4 signaling in the pathogen (44, 45). Consistent with TOR signaling being reduced in the *C. albicans oma1*Δ/Δ mutant, this strain shows significant enhancement of its resistance to phagocytic killing and its virulence.

Beyond the physiological relevance, our findings have biomedical importance. First, we identify Oma1 as a novel factor that integrates mitochondrial function with TOR signaling. Our data may provide explanations for some unexpected metabolic phenotypes in Oma1 knockout mice (51). Second, the enhanced rapamycin resistance and virulence observed in Oma1-deficient *C. albicans* cells reveals a new potential role of Oma1 as a therapeutic target/risk factor in systemic candidiasis. It is also possible that additional mitochondrial proteins, whose depletion can exert similar modulatory effects on TOR signaling, exist. Further studies are warranted to address these exciting questions.

ACKNOWLEDGMENTS

We thank Dennis Winge (University of Utah) and the members of the Khalimonchuk laboratory for critical comments. We also thank Christoph Schuller (University of Natural Resources, Austria) and Paul Herman (Ohio State University) for reagents. We acknowledge the expert technical assistance of Nataliya Zahayko. We also thank Donna MacCallum for help with the *Candida* virulence assays.

This research was supported by grants from the NIH (P30GM103335 and 5R01GM108975 [O.K.], GM071775-06 and GM105781-01 [A.B.], DK079209 [J.L.]), the U.K. Biotechnology and Biological Research Council (BB/K017365/1 [A.J.P.B.]), the U.K. Medical Research Council (MR/M026663/1 [A.J.P.B.]), and the European Research Council (C-2009-AdG-249793 [A.J.P.B.]).

We declare that we have no competing financial interests.

FUNDING INFORMATION

This work, including the efforts of Alistair J. P. Brown, was funded by Biotechnology and Biological Research Counsil (BB/K017365/1). This work, including the efforts of Oleh Khalimonchuk, was funded by HHS | National Institutes of Health (NIH) (5R01GM108975). This work, including the efforts of Oleh Khalimonchuk, was funded by HHS | National Institutes of Health (NIH) (P30GM103335).This work, including the efforts of Antoni Barrientos, was funded by HHS | National Institutes of Health (NIH) (GM071775-06). This work, including the efforts of Antoni Barrientos, was funded by HHS | National Institutes of Health (NIH) (GM105781-01). This work, including the efforts of Jaekwon Lee, was funded by HHS | National Institutes of Health (NIH) (DK079209). This work, including the efforts of Alistair J. P. Brown, was funded by Medical Research Council (MRC) (MR/M026663/1). This work, including the efforts of Alistair J. P. Brown, was funded by EC | European Research Council (ERC) (C-2009-AdG-249793).

REFERENCES

1. **Jazwinski SM, Kriete A.** 2012. The yeast retrograde response as a model of intracellular signaling of mitochondrial dysfunction. Front Physiol **3:**139. http://dx.doi.org/10.3389/fphys.2012.00139.
2. **Yun J, Finkel T.** 2014. Mitohormesis. Cell Metab **19:**757–766. http://dx.doi.org/10.1016/j.cmet.2014.01.011.
3. **Chandel NS.** 2014. Mitochondria as signaling organelles. BMC Biol **12:**34. http://dx.doi.org/10.1186/1741-7007-12-34.
4. **Swinnen E, Ghillebert R, Wilms T, Winderickx J.** 2014. Molecular mechanisms linking the evolutionary conserved TORC1-Sch9 nutrient signaling branch to lifespan regulation in *S. cerevisiae*. FEMS Yeast Res **14:**17–32. http://dx.doi.org/10.1111/1567-1364.12097.
5. **Balaban RS, Nemoto S, Finkel T.** 2005. Mitochondria, oxidants and aging. Cell **120:**483–495. http://dx.doi.org/10.1016/j.cell.2005.02.001.
6. **Schieber M, Chandel NS.** 2014. ROS function in redox signaling and oxidative stress. Curr Biol **24:**R453–R462. http://dx.doi.org/10.1016/j.cub.2014.03.034.
7. **Harman D.** 1972. The biologic clock: the mitochondria? J Am Geriatric Soc **20:**145–147. http://dx.doi.org/10.1111/j.1532-5415.1972.tb00787.x.
8. **Wallace DC.** 2005. A mitochondrial paradigm of metabolic and degenerative diseases, aging and cancer: a dawn for evolutionary medicine. Annu Rev Genet **39:**359–407. http://dx.doi.org/10.1146/annurev.genet.39.110304.095751.
9. **Gems D, Partridge L.** 2008. Stress-response hormesis and aging: "that which does not kill us makes us stronger". Cell Metab **7:**200–203. http://dx.doi.org/10.1016/j.cmet.2008.01.001.
10. **Cameroni E, Hulo N, Roosen J, Winderickx J, De Virgilio C.** 2004. The novel yeast PAS kinase Rim15 orchestrates G_0-associated antioxidant defence mechanisms. Cell Cycle **3:**462–468.
11. **Pan Y, Schroeder EA, Ocampo A, Barrientos A, Shadel GS.** 2011. Regulation of yeast chronological life span by TORC1 via adaptive mitochondrial ROS signaling. Cell Metab **13:**668–678. http://dx.doi.org/10.1016/j.cmet.2011.03.018.
12. **Anand R, Langer T, Baker MJ.** 2013. Proteolytic control of mitochondrial function and morphogenesis. Biochim Biophys Acta **1833:**195–204. http://dx.doi.org/10.1016/j.bbamcr.2012.06.025.
13. **Bohovych I, Donaldson G, Christianson S, Zahayko N, Khalimonchuk O.** 2014. Stress-triggered activation of the metalloprotease Oma1 involves its C-terminal region and is important for mitochondrial stress protection in yeast. J Biol Chem **289:**13259–13272. http://dx.doi.org/10.1074/jbc.M113.542910.
14. **Kaser M, Kambacheld M, Kisters-Woike B, Langer T.** 2003. Oma1, a novel membrane-bound metallopeptidase in mitochondria with activities overlapping with the m-AAA protease. J Biol Chem **278:**46414–46423. http://dx.doi.org/10.1074/jbc.M305584200.
15. **Khalimonchuk O, Jeong MY, Watts T, Ferris E, Winge DR.** 2012. Selective Oma1-mediated proteolysis of the Cox1 subunit of cytochrome oxidase in assembly mutants. J Biol Chem **287:**7289–7300. http://dx.doi.org/10.1074/jbc.M111.313148.
16. **Baker MJ, Lampe PA, Stojanovski D, Korwitz A, Anand R, Tatsuta T, Langer T.** 2014. Stress-induced OMA1 activation and autocatalytic turnover regulates OPA1-dependent mitochondrial dynamics. EMBO J **33:**578–593. http://dx.doi.org/10.1002/embj.201386474.
17. **Reiter W, Klopf E, De Wever V, Anrather D, Petryshyn A, Roetzer A, Niederacher G, Roitinger E, Dohnal I, Gorner W, Mechtler K, Brocard C, Schuller C, Ammerer G.** 2013. Yeast protein phosphatase 2A-Cdc55 regulates the transcriptional response to hyperosmolarity stress by regulating Msn2 and Msn4 chromatin recruitment. Mol Cell Biol **33:**1057–1072. http://dx.doi.org/10.1128/MCB.00834-12.
18. **Deminoff SJ, Howard SC, Hester A, Warner S, Herman PK.** 2006. Using substrate-binding variants of the cAMP-dependent protein kinase to identify novel targets and a kinase domain important for substrate interactions in *Saccharomyces cerevisiae*. Genetics **173:**1909–1917. http://dx.doi.org/10.1534/genetics.106.059238.
19. **MacCallum DM, Castillo L, Nather K, Munro CA, Brown AJ, Gow NA, Odds FC.** 2009. Property differences among the four major *Candida albicans* strain clades. Eukaryot Cell **8:**373–387. http://dx.doi.org/10.1128/EC.00387-08.
20. **Shahana S, Childers DS, Ballou ER, Bohovych I, Odds FC, Gow NA, Brown AJ.** 2014. New Clox ystems for rapid and efficient gene disruption in *Candida albicans*. PLoS One **9:**e100390. http://dx.doi.org/10.1371/journal.pone.0100390.
21. **Manukyan A, Abraham L, Dungrawala H, Scheider BL.** 2011. Synchronization of yeast. Methods Mol Biol **761:**173–200. http://dx.doi.org/10.1007/978-1-61779-182-6_12.
22. **Fradin C, De Groot P, MacCallum D, Schaller M, Klis F, Odds FC, Hube B.** 2005. Granulocytes govern the transcriptional response, morphology and proliferation of *Candida albicans* in human blood. Mol Microbiol **56:**397–415. http://dx.doi.org/10.1111/j.1365-2958.2005.04557.x.
23. **Bambach A, Fernandes MP, Ghosh A, Kruppa M, Alex D, Li D, Fonzi WA, Chauhan N, Sun N, Agrellos OA, Veresci AE, Rolfes RJ, Calderone R.** 2009. Goa1p of *Candida albicans* localizes to the mitochondria during

Downloaded from http://mcb.asm.org/ on September 9, 2016 by University of Aberdeen

stress and is required for mitochondrial function and virulence. Eukaryot Cell **8:**1706–1720. http://dx.doi.org/10.1128/EC.00066-09.
24. **Segal-Kischinevzky C, Rodarte-Murguia B, Valdes-Lopez V, Mendoza-Hernandez G, Gonzalez A, Alba-Lois L.** 2011. The euryhaline yeast Debariomyces hansenii has two catalase genes encoding enzymes with differential activity profile. Curr Microbiol **62:**933–943. http://dx.doi.org/10.1007/s00284-010-9806-z.
25. **Reinke A, Chen JC, Aronova S, Powers T.** 2006. Caffeine targets TOR complex I and provides evidence for a regulatory link between the FRB and kinase domains of Tor1p. J Biol Chem **281:**31616–31626. http://dx.doi.org/10.1074/jbc.M603107200.
26. **Endo A, Nakamura T, Ando A, Tokuyasu K, Shima J.** 2008. Genome-wide screening of the genes required for tolerance to vanillin, which is a potential inhibitor of bioethanol fermentation, in *Saccharomyces cerevisiae*. Biotechnol Biofuels **1:**3. http://dx.doi.org/10.1186/1754-6834-1-3.
27. **Li J, Kim SG, Blenis J.** 2014. Rapamycin: one drug, many effects. Cell Metab **19:**373–379. http://dx.doi.org/10.1016/j.cmet.2014.01.001.
28. **Xie MW, Jin F, Hwang H, Hwang S, Anand V, Duncan MC, Huang J.** 2005. Insights into TOR function and rapamycin response: chemical genomic profiling by using high-density cell array method. Proc Natl Acad Sci U S A **102:**7215–7220. http://dx.doi.org/10.1073/pnas.0500297102.
29. **Graef M, Nunnari J.** 2011. Mitochondria regulate autophagy by conserved signaling pathways. EMBO J **30:**2101–2114. http://dx.doi.org/10.1038/emboj.2011.104.
30. **Schmidt A, Beck T, Koller A, Kunz J, Hall MN.** 1998. The TOR nutrient signaling pathway phosphorylates NPR1 and inhibits turnover of the tryptophan permease. EMBO J **17:**6924–6931. http://dx.doi.org/10.1093/emboj/17.23.6924.
31. **Longo V, Shadel GS, Kaeberlein M, Kenendy B.** 2012. Replicative and chronological aging in *Saccharomyces cerevisiae*. Cell Metab **16:**18–31. http://dx.doi.org/10.1016/j.cmet.2012.06.002.
32. **Li H, Tsang CK, Watkins M, Bertram PG, Zheng XF.** 2006. Nutrient regulates Tor1 nuclear localization and association with rDNA promoter. Nature **442:**1058–1061. http://dx.doi.org/10.1038/nature05020.
33. **Wullschleger S, Loewith R, Oppliger W, Hall MN.** 2005. Molecular organization of target of rapamycin complex 2. J Biol Chem **280:**30697–30704. http://dx.doi.org/10.1074/jbc.M505553200.
34. **Godon C, Lagniel G, Lee J, Buhler JM, Kieffer S, Perrot M, Boucherie H, Toledano MB, Labarre J.** 1998. The H_2O_2 stimulon in S cerevisiae J Biol Chem **273:**22480–22489.
35. **Durchschlag E, Reiter W, Ammerer G, Schuller C.** 2004. Nuclear localization destabilizes the stress-regulated transcription factor Msn2. J Biol Chem **279:**55425–55432. http://dx.doi.org/10.1074/jbc.M407264200.
36. **Beck T, Hall MN.** 1999. The TOR signaling pathway controls nuclear localization of nutrient-regulated transcription factors. Nature **402:**689–692. http://dx.doi.org/10.1038/45287.
37. **Mesquita A, Weinberger M, Silva A, Sampaio-Marques B, Almeida B, Leao C, Costa V, Rodrigues V, Burhans WC, Ludovico P.** 2010. Caloric restriction or catalase inactivation extends yeast chronological lifespan by inducing H_2O_2 and superoxide dismutase activity. Proc Natl Acad Sci U S A **107:**15123–15128. http://dx.doi.org/10.1073/pnas.1004432107.
38. **Ocampo A, Liu J, Schroeder EA, Shadel GS, Barrientos A.** 2012. Mitochondrial respiratory thresholds regulate yeast chronological life span and its extension by caloric restriction. Cell Metab **16:**55–67. http://dx.doi.org/10.1016/j.cmet.2012.05.013.
39. **Schroeder EA, Raimundo N, Shadel GS.** 2013. Epigenetic silencing mediates mitochondria stress-induced longevity. Cell Metab **17:**954–964. http://dx.doi.org/10.1016/j.cmet.2013.04.003.
40. **Leadsham JE, Sanders G, Giannaki S, Bastow EL, Hutton R, Naemi WR, Breitenbach M, Gourlay CW.** 2013. Loss of cytochrome c oxidase promotes RAS-dependent ROS production from the ER resident NADPH oxidase, Yno1p, in yeast. Cell Metab **18:**279–286. http://dx.doi.org/10.1016/j.cmet.2013.07.005.
41. **Bohovych I, Fernandez MR, Rahn JJ, Stakley KD, Bestman JE, Anandhan A, Franco R, Claypool SM, Lewis RE, Chan SSL, Khalimonchuk O.** 2015. Metalloprotease OMA1 fine-tunes mitochondrial bioenergetic function and respiratory supercomplex stability. Sci Rep **5:**13989. http://dx.doi.org/10.1038/srep13989.
42. **Liu W, Zhao J, Li X, Li Y, Jiang L.** 2010. The protein kinase CaSch9p is required for the cell growth, filamentation and virulence in the human fungal pathogen *C. albicans*. FEMS Yeast Res **10:**462–470. http://dx.doi.org/10.1111/j.1567-1364.2010.00617.x.
43. **Sullivan DJ, Moran GP.** 2011. Differential virulence in of *C. albicans* and *C. dubliniensis*: a role for Tor1 kinase? Virulence **2:**77–81. http://dx.doi.org/10.4161/viru.2.1.15002.
44. **Nicholls S, Straffon M, Enjalbert B, Nantel A, Macaskill S, Whiteway M, Brown AJ.** 2004. Msn2- and Msn4-like transcription factors play no obvious roles in the stress responses of the fungal pathogen *C. albicans*. Eukaryot Cell **3:**1111–1123. http://dx.doi.org/10.1128/EC.3.5.1111-1123.2004.
45. **Brown AJP, Odds FC, Gow NAR.** 2007. Infection-related gene expression in *Candida albicans*. Curr Opin Microbiol **10:**307–313. http://dx.doi.org/10.1016/j.mib.2007.04.001.
46. **Junqueira JC.** 2012. *Galleria mellonella* as a model host for human pathogens. Virulence **3:**474–476. http://dx.doi.org/10.4161/viru.22493.
47. **Zoncu R, Efeyan A, Sabatini DM.** 2011. mTOR: from growth signal integration to cancer, diabetes and ageing. Nat Rev Mol Cell Biol **12:**21–35. http://dx.doi.org/10.1038/nrm3025.
48. **Wang Y, Hekimi S.** 2015. Mitochondrial dysfunction and longevity in animals: untangling the knot. Science **350:**1204–1207. http://dx.doi.org/10.1126/science.aac4357.
49. **Okazaki S, Naganuma A, Kuge S.** 2005. Peroxiredoxin-mediated redox regulation of the nuclear localization of Yap1, a transcription factor in budding yeast. Antioxid Redox Signal **7:**327–334. http://dx.doi.org/10.1089/ars.2005.7.327.
50. **Molin M, Yang J, Hanzen S, Toledano MB, Labarre J, Nystrom T.** 2011. Life span extension and H_2O_2 resistance elicited by caloric restriction require the peroxiredoxin Tsa1 in *S. cerevisiae*. Mol Cell **43:**823–833. http://dx.doi.org/10.1016/j.molcel.2011.07.027.
51. **Quiros PM, Ramsay AJ, Sala D, Fernandez-Vizarra E, Rodriguez F, Peinado JR, Fernandez-Garcia MS, Vega JA, Enriquez JA, Zorzano A, Lopez-Otin C.** 2012. Loss of mitochondrial protease OMA1 alters processing of the GTPase OPA1 and causes obesity and defective thermogenesis in mice. EMBO J **31:**2117–2133. http://dx.doi.org/10.1038/emboj.2012.70.

Downloaded from http://mcb.asm.org/ on September 9, 2016 by University of Aberdeen